

Quantum Otto engine with quantum correlations

Yang Xiao¹, Dehua Liu¹, Jizhou He¹, Yongli Ma^{2,*}, Zhaoqi Wu³, and Jianhui Wang^{1,2†}

¹ *Department of Physics, Nanchang University, Nanchang 330031, China*

² *State Key Laboratory of Surface Physics and Department of Physics, Fudan University, Shanghai 200433, China*

³ *School of Mathematics and Computer Science, Nanchang University, Nanchang 330031, China*

(Dated: November 24, 2022)

We theoretically propose and investigate a quantum Otto engine that is working with a single-mode radiation field inside an optical cavity and alternatively driven by a hot and a cold reservoir, where the hot reservoir is realized by using a beam of thermally entangled pairs of two-level atoms that resonantly interacts with the cavity, and the cold one is made of a collection of noninteracting boson modes. In terms of the quantum discord of the pair of atoms, we derive the analytical expressions for the performance parameters (power and efficiency) and stability measure (coefficient of variation for power). We show that quantum discord boosts the performance and efficiency of the quantum engine, and even may change the operation mode. We also demonstrate that quantum discord improves the stability of machine by decreasing the coefficient of variation for power which satisfies the generalized thermodynamic uncertainty relation. Finally, we find that these results can be transferred to another quantum Otto engine model, where the optical cavity is alternatively coupled to a hot thermal bosonic bath and to a beam of pairs of the two correlated atoms that play the role of a cold reservoir.

I. INTRODUCTION

The presence of nonclassical correlations is one of the most intriguing signatures of the non-classicality for a quantum state. These correlations have been considered as a type of resource in some quantum tasks such as quantum computation and quantum information processing [1–8]. Quantum discord, which usually quantifies nonclassical correlations, is more general than entanglement [7, 9]. It is defined as the difference between quantum mutual information and classical correlations in a system [7, 10, 11]. Although quantum discord is not always larger than the quantum entanglement, it may be nonzero even for separable states in the absence of entanglement [2, 10, 12, 13]. The quantum discord is a good figure of merit for characterizing quantum resource not only in quantum information theory, but also in the field of quantum thermodynamics [14–17] with a focus on quantum thermal machines [15, 16].

Classical heat engines convert thermal resources into mechanical work, of which the thermodynamic efficiency is bounded by the Carnot bound [18, 19]. Unlike in the classical case, in quantum realm not only the working substance but also the heat reservoirs may be composed of finite-size systems which can be prepared in quantum states without classical analogues. When playing the role of the reservoirs, these finite-dimension systems give rise to a non-thermal scenario where the heat engines outperform the classical analogs [20–22]. Additionally, the fluctuations in quantum heat engines can not be neglected as both work and heat are stochastic and fluctuating [23–30]. Quantum heat engines op-

erating with out-of-equilibrium reservoirs, which may be squeezed [20, 21, 31–38], quantum coherent [39–45], quantum-measurement-induced [46–51], and nonclassical correlated [5, 6, 52], were theoretically investigated and experimentally performed in either finite-time or quasistatic operation mode. These engines outperforming their classical counterparts may be different cycle models, such as the Carnot cycle [40, 44], Otto cycle [20, 21, 32], and Stirling cycle [38], etc. A photo-Carnot engine introduced by Scully and his coworkers [44] was extended by including quantum correlations to explore the thermodynamic efficiency beyond the Carnot limit [13]. It is well known that, except for the reversible Carnot engine working between two thermal reservoirs, the performance for the heat engines is always model-dependent, irrespective of thermal or nonthermal reservoirs.

In the present paper, aiming at using quantum correlations for thermodynamic applications, we propose a quantum Otto engine, unexplored so far, which is working with a single-mode optical cavity and driven by an out-of-equilibrium reservoir with quantum correlations. Besides two thermodynamic adiabatic processes, the engine consists of a hot and a cold isochoric stroke, where the optical cavity is weakly coupled to a thermal reservoir during the cold isochore and it resonantly interacts with one of the pair of correlated atoms along the hot isochore. We examine the finite-time performance and power fluctuations by changing the quantum discord. We show that quantum discord (i) can change the operation mode, e.g., a thermal device expected to operate as a refrigerator in the absence of quantum discord may operate as a heat engine once the nonclassical correlations are present, (ii) increases work extraction and thermodynamic efficiency but decreasing the relative power fluctuations, with the latter satisfying the generalized thermodynamic uncertainty relation [53], and (iii) enables the finite-time engine to operate at the efficiency beyond the Carnot limit.

*Electronic address: yhma@ncu.edu.cn

†Electronic address: wangjianhui@ncu.edu.cn

We finally demonstrate that, the result is applicable to an alternative quantum Otto cycle, where the hot reservoir is composed of quantized boson modes and the cold reservoir consists of the pairs of two-level atoms sequentially passing through the optical cavity.

This paper is organized as follows. In Sec. II we briefly review the quantum discord different from entanglement. We then discuss a quantum Otto engine cycle in Sec. III, where the effects of quantum discord on the performance and fluctuations are discussed. We finally make discussions and conclusions in Sec. IV.

II. QUANTUM ENTANGLEMENT AND DISCORD

Let us consider the Hamiltonian of two identical spin-1/2 atoms with frequency ω via a XY Heisenberg interaction ($\hbar \equiv 1$) [54]:

$$H = \frac{\omega}{2}(\sigma_1 + \sigma_2) + \xi(\sigma_1^+ \sigma_2^- + \sigma_1^- \sigma_2^+), \quad (1)$$

where ξ is the controllable strength of the interaction. The operator $\sigma_j^+ = (\sigma_j^-)^\dagger = |e\rangle_{jj}\langle g| = \frac{1}{2}(\sigma_j^x + i\sigma_j^y)$, $\sigma_j^z = |e\rangle_{jj}\langle e| - |g\rangle_{jj}\langle g|$, where $|g\rangle_j$, $|e\rangle_j$, and σ_j^α ($\alpha = x, y, z$) are the ground state, excited state, and Pauli matrices for atom j (with $j = 1, 2$), respectively. The eigenvalues E_i and the corresponding eigenvectors $|\Psi_i\rangle$ of the Hamiltonian (1) can be calculated as

$$\begin{aligned} E_1 &= -E_4 = \omega, |\Psi_1\rangle = |ee\rangle, |\Psi_4\rangle = |gg\rangle, \\ E_2 &= -E_3 = \xi, |\Psi_2\rangle = \frac{\sqrt{2}}{2}(|ge\rangle + |eg\rangle), \\ |\Psi_3\rangle &= \frac{\sqrt{2}}{2}(-|ge\rangle + |eg\rangle). \end{aligned} \quad (2)$$

When the two-atom system is at thermal equilibrium with inverse temperature β , the density operator can be determined by $\rho_{12} = e^{-\beta H}/Z$, with the canonical partition function $Z = \text{Tr}(e^{-\beta H})$. It follows, using Eqs. (1) and (2), the thermal state of the system can be described by

$$\begin{aligned} \rho_{12} &= \frac{1}{Z}(e^{-\beta\omega}|\Psi_1\rangle\langle\Psi_1| + e^{-\beta\xi}|\Psi_2\rangle\langle\Psi_2| \\ &+ e^{\beta\xi}|\Psi_3\rangle\langle\Psi_3| + e^{\beta\omega}|\Psi_4\rangle\langle\Psi_4|), \end{aligned} \quad (3)$$

where the partition function $Z = 2[\cosh(\beta\omega) + \cosh(\beta\xi)]$. To describe the entanglement between the two atoms, one introduces the concurrence [55, 56] which can be evaluated by Eq. (3) to be written in closed form:

$$\mathcal{C}(\rho_{12}) = \max\left\{0, \frac{\sinh(\beta\xi) - 1}{\cosh(\beta\omega) + \sinh(\beta\xi)}\right\}. \quad (4)$$

While for $\beta\xi \leq \text{arcsinh}(1)$ the concurrence is zero and the mixture is separable due to vanishing entanglement, for $\beta\xi > \text{arcsinh}(1) \approx 0.88$, the concurrence is positive and the entanglement between the two atoms is

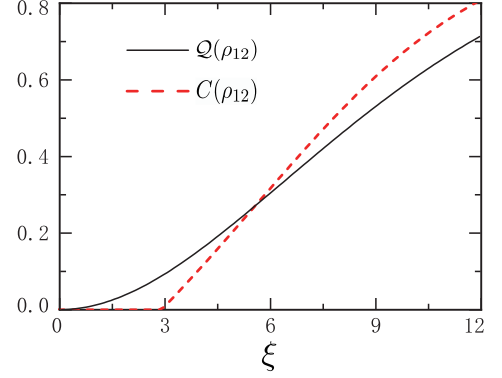


FIG. 1: Quantum discord and concurrence as a function of interaction strength with parameters $\omega = 6$ and $\beta = 0.3$.

non-negligible. This implies that, the thermal state (3) would be entangled in the low-temperature and/or strong-coupling case.

The quantum discord, defined as the difference between quantum mutual information $\mathcal{I}(\rho_{12})$ and classical correlations $\mathcal{J}(\rho_{12})$ [10, 11], takes the form of

$$\mathcal{Q}(\rho_{12}) := \mathcal{I}(\rho_{12}) - \mathcal{J}(\rho_{12}). \quad (5)$$

The quantum mutual information is given by $\mathcal{I}(\rho_{12}) = S(\rho_1) + S(\rho_2) - S(\rho_{12})$, where $S(\rho) = -\text{Tr}[\rho \log_2 \rho]$ is the von Neumann entropy, $\rho_{1(2)} = \text{Tr}_{2(1)}(\rho_{12})$ is the reduced density matrix of atom 1(2). In order to describe the classical correlations $\mathcal{J}(\rho_{12})$, the measurement basis $\{B_k\}$ is introduced to describe a von Neumann measurement for atom 2 only. The conditional density operator ρ_1^k associated with the measurement result k is then given by $\rho_1^k = (I \otimes B_k)\rho_{12}(I \otimes B_k)/p_k$, where the probability $p_k = \text{Tr}[(I \otimes B_k)\rho_{12}(I \otimes B_k)]$. The quantum conditional entropy with respect to this measurement basis is $S(\rho_1|\{B_k\}) = \sum_k p_k S(\rho_1^k)$, and then the classical correlations are determined by $\mathcal{J}(\rho_{12}) = \sup_{\{B_k\}} [S(\rho_1) - S(\rho_1|\{B_k\})]$ [57–59]. Using the parameterized basis $\{B_k\} = \{\cos\theta|g\rangle - \sin\theta|e\rangle, -\sin\theta|g\rangle - \cos\theta|e\rangle\}$, it follows that the minimum of the discord is reached at $\theta = \pi/4$ [13], which reads

$$\begin{aligned} \mathcal{Q}(\rho_{12}) &= -\frac{1}{\ln(2)}\{2(\beta\xi)\rho_{nd} + \rho_d \ln[Z^2(\rho_g + \rho_d)(\rho_e + \rho_d)] \\ &+ \sum_{\alpha=g,e} \rho_\alpha \ln\left(\frac{\rho_\alpha + \rho_d}{\rho_\alpha}\right) + \sum_{\epsilon=\pm} \Phi_\epsilon \ln \Phi_\epsilon\}, \end{aligned} \quad (6)$$

where $\rho_g = \langle gg|\rho_{12}|gg\rangle = Z^{-1}\exp(\beta\omega)$, $\rho_e = \langle ee|\rho_{12}|ee\rangle = Z^{-1}\exp(-\beta\omega)$, $\rho_d = \langle eg|\rho_{12}|eg\rangle = Z^{-1}\cosh(\beta\xi)$, $\rho_{nd} = \langle eg|\rho_{12}|ge\rangle = \langle ge|\rho_{12}|eg\rangle = -Z^{-1}\sinh(\beta\xi)$, $\Phi_\epsilon = (1 + \epsilon\sqrt{(\rho_e - \rho_g)^2 + 4\rho_{nd}^2})/2$. In the limit of high temperature and/or weakly coupling, where $\beta\xi \ll 1$, Eq. (6) simplifies to $\mathcal{Q}(\rho_{12}) \simeq (\beta\xi)^2/(8\ln 2)$.

In Fig. (1) we plot the quantum discord $\mathcal{C}(\rho_{12})$ and concurrence $\mathcal{Q}(\rho_{12})$, Eqs. (4) and (6), as a function of

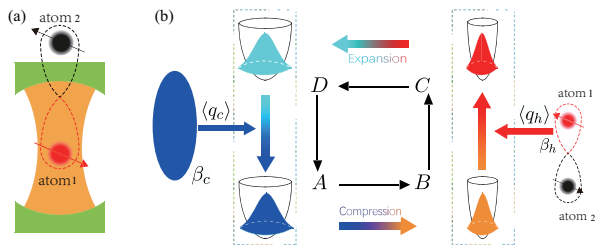


FIG. 2: (a) Sketch of a single-mode optical cavity coupled to one of two correlated atoms. (b) Illustration of a finite-time quantum Otto engine. During the first stroke $A \rightarrow B$, the working substance at the thermal state undergoes a unitary compression in time period τ_{ch} , and its Hamiltonian changes from $H(\omega_c)$ to $H(\omega_h)$. In the second stroke $B \rightarrow C$, the optical cavity for fixed frequency ($\omega = \omega_h$) is coupled to one of two correlated atoms with inverse temperature β_h , and it reaches the stationary state at the end of this stroke. The coupling is realized by sending this atom to pass through the optical cavity. The third stroke $C \rightarrow D$ is a unitary expansion where the Hamiltonian evolves from $H(\omega_h)$ to $H(\omega_c)$ during time τ_{hc} . In the cooling stroke $D \rightarrow A$, the working substance with constant frequency ω_c in contact with the cold thermal bath of inverse temperature β_c relaxes to the thermal state by closing the cycle. The average heats absorbed by the working system along the hot and cold isochoric strokes are denoted by $\langle q_h \rangle$ and $\langle q_c \rangle$, respectively. We assume the time spent on the isochoric stroke to be much shorter than that on the unitary stroke [20] and the time for completing a cycle is $\tau_{cyc} = \tau_{ch} + \tau_{hc}$.

interaction strength ξ . Both of quantum discord and concurrence decrease as interaction strength decreases and they vanish in the absence of inter-particle interaction, as expected. Quite interestingly, while the concurrence vanishes when the interaction strength is quite small, the quantum discord is zero only in the absence of interactions between two atoms. It is therefore indicated that the quantum discord may be nonzero even when the nonentangled states are separable. In what follows, we will use quantum discord $\mathcal{Q}(\rho_{12})$ rather than the concurrence $\mathcal{C}(\rho_{12})$ to capture the information of the correlations of the two-atom system.

III. QUANTUM OTTO ENGINE

A. Four consecutive strokes in a machine cycle

We consider a quantum engine cycle that uses a single mode of the quantized radiation in an optical cavity as its working substance and operates between a hot and a cold heat reservoir. While in the cold isochoric process the thermal bath is composed of an infinite collection of noninteracting bosonic modes, during the hot isochoric stroke the optical cavity resonantly interacts with a beam of thermally entangles pairs of two-level atoms [see Fig. 2(a)] that play the role of the hot non-thermal reservoir.

The interaction of the cavity with these atoms is realized by sending only one of a pair of atoms to pass through the cavity, which means that only one of the atoms interacts with the radiation field [13]. The engine model under consideration as a quantum version of Otto cycle is sketched in Fig. 2(b). It consists of two unitary strokes $A \rightarrow B$ and $C \rightarrow D$, where the system is isolated from two heat reservoirs, and two isochoric branches $B \rightarrow C$ and $D \rightarrow A$, along each of which the optical cavity with constant Hamiltonian is weakly coupled to the hot or cold reservoir. We now describe the four consecutive steps of the Otto engine cycle as follows.

(i) Unitary compression $A \rightarrow B$. The system is isolated from the heat reservoir and undergoes a unitary compression in time τ_{ch} . Its Hamiltonian is changed from $H(\omega_c) = \omega_c(\hat{a}^\dagger \hat{a} + 1/2)$ to $H(\omega_h) = \omega_h(\hat{a}^\dagger \hat{a} + 1/2)$ with driving function $\omega_{ch}(t) = \omega_c \omega_h \tau_{ch} / [(\omega_c - \omega_h)t + \omega_h \tau_{ch}]$ where \hat{a} and \hat{a}^\dagger are the annihilation and the creation operators of the oscillator, respectively. Since no heat is exchanged, the change of the system internal energy is equal to the work done on the system. We use two-projective-measurement scheme [26] to calculate the probability distribution of quantum work as

$$p(w) = \sum_{n,m} \delta[w_{ch} - (\varepsilon_m^h - \varepsilon_n^c)] p_{n \rightarrow m}^{ch} p_n^A, \quad (7)$$

where ε_n^c and ε_m^h are the measured energies at the beginning and the end of this stroke, respectively. Here, p_n^A is the initial occupation probability, and $p_{n \rightarrow m}^{ch} = |\langle n | U_{ch} | m \rangle|^2$ with the unitary operator U_{ch} , is the transition probability between the instantaneous eigenstates $|n\rangle$ and $|m\rangle$.

(ii) Isochoric heating $B \rightarrow C$. The Hamiltonian of the single radiation mode in the cavity is constant with fixed frequency ω_h . Thus, the stochastic heat injection is equivalent to the increase of the system eigenenergy with zero work. We can write the probability distribution for the heat absorbed during this stroke as

$$p(q_h | w_{ch}) = \sum_{k,l} \delta[q_h - (\varepsilon_l^h - \varepsilon_k^h)] p_{k \rightarrow l}^B p_k^B, \quad (8)$$

where ε_k^h and ε_l^h are the measured energies at the beginning and the end of heating stroke, respectively. $p_k^B = \delta_{km}$ is the probability when system is in eigenstate $|m\rangle$ after second protective measurement. The transition probability $p_{k \rightarrow l}^B = |\langle l | U_h | k \rangle|^2 = \langle l | U_h \rho_{\text{mea}}^{\tau_{ch}} U_h^\dagger | l \rangle = \langle l | \rho^C | l \rangle = p_l^C$, where U_h is the propagator of this stroke, $\rho_{\text{mea}}^{\tau_{ch}}$ is the density operator after second measurement, and p_l^C is the probability that the system is in $|l\rangle$ state at the end of this stroke.

For the hot isochoric stroke, we consider the case where only one atom of the correlated pair with constant inverse temperature β_h is sent to pass through the cavity. The atom that passes through the optical cavity interacts with the cavity via a resonant Jaynes-Cummings coupling, $H^{int} = -\gamma(\hat{a}\sigma^+ + \hat{a}^\dagger\sigma^-)$ [60], with coupling constant γ . When an ensemble of many atoms are sent

to the optical cavity, the dynamics of cavity state can be described by [13, 61]

$$\begin{aligned} \frac{d\rho_t}{dt} = & r_1^h(\gamma\tau)^2(a^\dagger\rho_t a - \frac{1}{2}aa^\dagger\rho_t - \frac{1}{2}\rho_t aa^\dagger) \\ & + r_2^h(\gamma\tau)^2(a\rho_t a^\dagger - \frac{1}{2}a^\dagger a\rho_t - \frac{1}{2}\rho_t a^\dagger a), \end{aligned} \quad (9)$$

where τ is the time spent by the atoms inside the cavity. The coefficients r_1^h and r_2^h are the arrival rates for atoms in the excited and ground state, respectively, and thus they are associated with the probabilities of emission and absorption of a photon in the cavity. These two are determined according to $r_1^h = \rho_e^h + \rho_d^h$ and $r_2^h = \rho_g^h + \rho_d^h$ with $\rho_e^h = \exp(-\beta_h\omega_h)/[2\cosh(\beta_h\omega_h) + 2\cosh(\beta_h\xi)]$, $\rho_g^h = \exp(\beta_h\omega_h)/[2\cosh(\beta_h\omega_h) + 2\cosh(\beta_h\xi)]$, and $\rho_d^h = \cosh(\beta_h\xi)/[2\cosh(\beta_h\omega_h) + 2\cosh(\beta_h\xi)]$. The optical cavity as the working substance is allowed to relax to the stationary state at the end of hot isochoric stroke, and the time duration of this stroke is assumed to be much shorter than the duration of the unitary stroke. The asymptotic steady-state solution of Eq. (9), which describes the stationary state of the optical cavity, is obtained as

$$\rho^{ss} = (1 - e^{-\beta_h^{\text{eff}}\omega_h})e^{-\beta_h^{\text{eff}}\omega_h a^\dagger a}, \quad (10)$$

where we have introduced β_h^{eff} to denote the effective inverse temperature of the optical cavity. The condition of detailed balance, $\exp(-\beta_h^{\text{eff}}\omega_h) = r_1^h/r_2^h$, gives rise to

$$\beta_h^{\text{eff}} = \beta_h - \frac{1}{\omega_h} \ln \frac{1 + e^{\beta_h\omega_h} \cosh(\beta_h\xi)}{e^{\beta_h\omega_h} + \cosh(\beta_h\xi)}, \quad (11)$$

which can be simplified to $\beta_h^{\text{eff}}/\beta_h \simeq 1 - (\beta_h\xi)^2/4 = 1 - 2Q(\rho_{12})\ln 2$ in the limit of high temperature or/and weak coupling.

(iii) Unitary expansion $C \rightarrow D$. The optical cavity is isolated again from heat reservoir and undergoes a unitary expansion in time period τ_{hc} with driving function $\omega_{hc}(t) = \omega_c\omega_h\tau_{hc}/[(\omega_h - \omega_c)(t - \tau_{ch}) + \omega_c\tau_{hc}]$. Since this stroke can be accomplished by reversing the protocol used in the above compression process, we set $\tau_{\text{dri}} \equiv \tau_{hc} = \tau_{ch}$ to have $\omega_{hc}(t) = \omega_{ch}(2\tau_{\text{dri}} - t)$. In this stroke no heat is exchanged, the change of the system internal energy is equal to the work done on the system. Using two-projective-measurement scheme again, the probability distribution of stochastic work is

$$p(w_{hc}|w_{ch}, q_h) = \sum_{i,j} \delta[w_{hc} - (\varepsilon_j^c - \varepsilon_i^h)] p_{i \rightarrow j}^{hc} p_i^C, \quad (12)$$

where $p_i^C = \delta_{il}$ is the probability when the optical cavity is in eigenstate $|l\rangle$ after the third protective measurement. $p_{i \rightarrow j}^{hc} = |\langle j|U_{hc}|i\rangle|^2$ is the transition probability between the instantaneous eigenstates $|i\rangle$ and $|j\rangle$ where U_{hc} is corresponding unitary operator.

(iv) Isochoric cooling $D \rightarrow A$. The system, with constant Hamiltonian $H(\omega) = H(\omega_c)$, is coupled to a thermal reservoir of constant inverse temperature β_c in time

duration much smaller than the adiabatic driving time τ_{dri} . The system reaches thermal equilibrium with the heat reservoir at the ending point of the cold isochore, and the state of the system at this point is given by $\rho_0 = e^{-\beta_c H(\omega_c)}/\text{Tr}[e^{-\beta_c H(\omega_c)}]$.

After a single cycle, the joint distribution of total work w and heat injection q_h can be calculated by combining Eqs. (7), (8) and (12) to arrive at

$$\begin{aligned} p(w, q_h) = & \sum_{n,m,i,j} \delta(w + \varepsilon_n^c - \varepsilon_j^c + \varepsilon_i^h - \varepsilon_m^h) \\ & \times \delta(q_h - \varepsilon_i^h + \varepsilon_m^h) |\langle m|U_{ch}|n\rangle|^2 |\langle j|U_{hc}|i\rangle|^2 \\ & \times \frac{e^{-\beta_c \varepsilon_n^c} e^{-\beta_h^{\text{eff}} \varepsilon_i^h}}{Z_c Z_h}, \end{aligned} \quad (13)$$

with the partition functions $Z_c = \text{Tr}[e^{-\beta_c H(\omega_c)}]$ and $Z_h = \text{Tr}[e^{-\beta_h^{\text{eff}} H(\omega_h)}]$.

B. Machine performance and fluctuations

To determine the statistics of work and heat, the characteristic function of the joint distribution function $p(w, q_h)$ (13), $G(u, v) \equiv \int \int p(w, q_h) e^{-ivq_h - iuw} dw dq_h$, can be obtained as [62, 63],

$$G(u, v) = \langle e^{-ivq_h - iuw} \rangle = \frac{G_c G_h}{1 + \phi} \quad (14)$$

where

$$G_c = \frac{e^{\beta_c \omega_c} - 1}{\sqrt{r_\phi \cosh(\beta_c \omega_c + iv_0) + \cosh(\beta_c \omega_c + iu_0) - 2}}, \quad (15)$$

and

$$G_h = \frac{e^{\beta_h^{\text{eff}} \omega_h} - 1}{\sqrt{r_\phi \cos(v_0 - i\beta_h^{\text{eff}} \omega_h) + \cos(i\beta_h^{\text{eff}} \omega_h + u_0) - 2}}. \quad (16)$$

Here we have used $u_0 = u(\omega_c - \omega_h) + v\omega_h$, $v_0 = u(\omega_c + \omega_h) - v\omega_h$, and $r_\phi = (1 - \phi)/(1 + \phi)$. The parameter ϕ is given by

$$\phi \equiv 1 + \frac{1 - \cos[\sqrt{\zeta - 1} \ln(\omega_h/\omega_c)]}{\zeta - 1}, \quad (17)$$

with $\zeta = [2\tau_{\text{dri}}\omega_c\omega_h/(\omega_h - \omega_c)]^2$, and it is called the nonadiabatic factor. As expected, the nonadiabatic factor would become equivalent to 1 in the quantum adiabatic case where τ_{dri} is long enough.

The average and the variance of the work as well as the average heat injection can be explicitly obtained,

$$\begin{aligned} \langle w \rangle = & -i \left. \frac{\partial \ln G(u, v)}{\partial u} \right|_{u=v=0} \\ = & \omega_h (\phi \langle n_c^{eq} \rangle - \langle n_h^{ss} \rangle) + \omega_c (\phi \langle n_h^{ss} \rangle - \langle n_c^{eq} \rangle), \end{aligned} \quad (18)$$

$$\begin{aligned}
\delta w^2 &= \langle w^2 \rangle - \langle w \rangle^2 = -\left. \frac{\partial^2 \ln G(u, v)}{\partial u^2} \right|_{u=v=0} \\
&= \omega_h^2 \left[-\frac{1}{2} + (2\phi^2 - 1) \langle n_c^{eq} \rangle^2 + \langle n_h^{ss} \rangle^2 \right] \\
&+ \omega_c^2 \left[-\frac{1}{2} + \langle n_c^{eq} \rangle^2 + (2\phi^2 - 1) \langle n_h^{ss} \rangle^2 \right] \quad (19) \\
&+ \omega_h \omega_c \phi (1 - 2 \langle n_c^{eq} \rangle^2 - 2 \langle n_h^{ss} \rangle^2),
\end{aligned}$$

$$\langle q_h \rangle = -i \left. \frac{\partial \ln G(u, v)}{\partial v} \right|_{u=v=0} = \omega_h (\langle n_h^{ss} \rangle - \phi \langle n_c^{eq} \rangle), \quad (20)$$

respectively, where we have used $\langle n_c^{eq} \rangle = \coth(\beta_c \omega_c / 2) / 2$ and $\langle n_h^{ss} \rangle = \coth(\beta_h^{\text{eff}} \omega_h / 2) / 2$ to denote the excitation numbers of the cavity with the cold thermal and the hot nonthermal reservoirs, respectively. The heat absorbed by the system from the cold reservoir is set by the heat injection $\langle q_h \rangle$ and the average output work $\langle w \rangle$, $\langle q_c \rangle = -\langle w \rangle - \langle q_h \rangle$ [see also Fig. 2(b)].

The average values of work and heat injection depend on the quantum discord which enters into $\langle n_h^{ss} \rangle$ and, under this condition, even the operation mode can change when quantum discord is involved. Noteworthy, the mean work (18) can be split into a sum of two parts: $-\langle w \rangle = \langle w_{\text{adi}} \rangle - \langle w_{\text{fric}} \rangle$, where one part $w_{\text{adi}} = (\omega_h - \omega_c)(n_h^{ss} - n_c^{eq})$ is the mean work in quantum adiabatic case, and the other part $\langle w_{\text{fric}} \rangle = (\phi - 1)(\omega_h n_c^{eq} + \omega_c n_h^{ss})$ is the frictional work due to diabatic transitions along the two unitary driven processes.

Both the mean work $-\langle w \rangle$ and mean heat injection $\langle q_h \rangle$ are increased by increasing quantum discord $\mathcal{Q}(\rho_{12})$. When the control parameters including $\omega_{c,h}$ and $\beta_{h,c}$ are given, gradually increasing $\mathcal{Q}(\rho_{12})$ results in that the following three consecutive operation modes (upper panel, Fig. 3): (i) the refrigerator ($-\langle w \rangle < 0$, $\langle q_h \rangle < 0$, $\langle q_c \rangle > 0$), (ii) the heater ($-\langle w \rangle < 0$, $\langle q_c \rangle < 0$), and (iii) the heat engine ($-\langle w \rangle > 0$, $\langle q_h \rangle > 0$, $\langle q_c \rangle < 0$). For the heater, whereas the heat must flow into the cold reservoir, $\langle q_c \rangle < 0$, the average heat injection $\langle q_h \rangle$ can be an arbitrary real number, with no useful work extracted, $-\langle w \rangle \leq 0$. When operating as a refrigerator, the machine absorbs heat from the cold reservoir, which entails $\langle q_c \rangle > 0$, and releases the heat into the hot reservoir, so that $\langle q_h \rangle < 0$, while work should be consumed, $-\langle w \rangle < 0$. For the refrigerator, its coefficient of performance is defined as the ratio of cooling load to work input, namely, $\varepsilon = \langle q_c \rangle / \langle w \rangle$, which is positive (see lower panel in Fig. 3).

The thermodynamic efficiency, defined by $\eta_{th} = -\langle w \rangle / \langle q_h \rangle$, where $\langle w \rangle$ and $\langle q_h \rangle$ were given by Eqs. (18) and (20), can be obtained as

$$\eta_{th} = 1 - \frac{\omega_c}{\omega_h} - \frac{\omega_c (\phi - 1) (n_h^{ss} + \langle n_c^{eq} \rangle)}{\omega_h (\langle n_h^{ss} \rangle - \phi \langle n_c^{eq} \rangle)}, \quad (21)$$

which reduces to the so-called Otto efficiency, $\eta_O = 1 - \omega_c / \omega_h$, if two unitary strokes are quantum adiabatic, irrespective of existence of correlations between two atoms. The efficiency η_{th} as a function of $\mathcal{Q}(\rho_{12})$

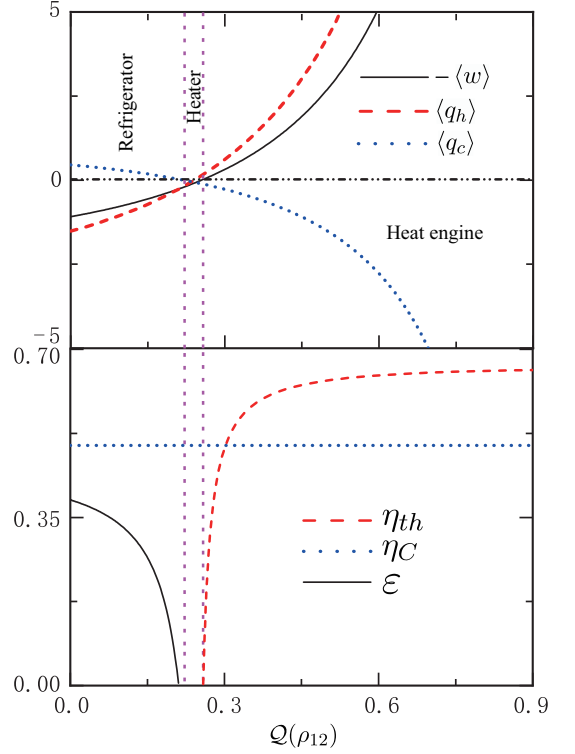


FIG. 3: Work output and heats absorbed by the system (upper panel), and thermodynamic efficiency (lower panel) as a function of quantum discord. The parameters are $\beta_c = 0.6$, $\beta_h = 0.3$, $\omega_h = 6$, $\omega_c = 2$, and driving time $\tau_{\text{dri}} = 0.8$.

is illustrated by the lower panel of Fig. 3. With increasing quantum discord $\mathcal{Q}(\rho_{12})$, the efficiency η_{th} monotonically increases and it may surpass the Carnot efficiency $\eta_C = 1 - \beta_h / \beta_c$. The efficiency (21) can be rewritten as $\eta_{th} = \eta_C^{\text{gen}} - \langle \sigma \rangle / (\beta_h^{\text{eff}} \langle q_h \rangle)$, where $\eta_C^{\text{gen}} = 1 - \beta_h^{\text{eff}} / \beta_c$ is the so-called generalized Carnot efficiency and $\langle \sigma \rangle = -\beta_h^{\text{eff}} \langle q_h \rangle - \beta_c \langle q_c \rangle \geq 0$ is the average entropy production of the heat engine in a single cycle [64]. We therefore conclude that the thermodynamic efficiency may be larger than the Carnot value, but it satisfies the second law of thermodynamics as it must be smaller than the generalized Carnot value.

The nonadiabatic factor (17) depends on the driving time τ_{dri} , and thus the efficiency η_{th} is a function of not only the quantum discord $\mathcal{Q}(\rho_{12})$ but also the driving time τ_{dri} . When the driven stroke speeds down, the nonadiabatic factor decreases, although not monotonically, and approaches the lower bound, $\phi = 1$, for large τ_{dri} [see the insert of Fig. 4(a)]. As a consequence, the efficiency increases very quickly at first, then levels off and becomes asymptotic to the Otto efficiency [see Fig. 4(a)]. In addition to the efficiency, the power output, $P = -\langle w \rangle / \tau_{\text{cyc}}$, is another an important measure of the machine performance. The power output as a function of τ_{dri} behaves similarly to the efficiency [see Fig. 4(b)]. The power is initially increasing fast to approach the

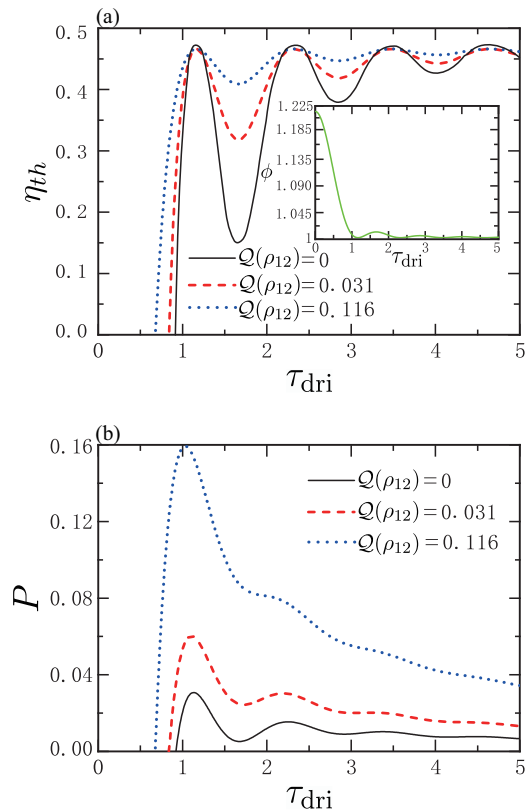


FIG. 4: (a) Thermodynamics efficiency and (b) power output as a function of driving time with different values of quantum discord. The inset in (a) shows the nonadiabatic factor as a function of driving time. The parameters are $\beta_c = 0.6$, $\beta_h = 0.3$, $\omega_h = 3.8$, and $\omega_c = 2$.

maximum value and then non-monotonically decreasing. In physical terms, when the driving time τ_{dri} increases, the frictional work $\langle w_{fri} \rangle$ quickly drops, and then very slowly decreases to zero.

We also observe from Figs. 4(a) and 4(b) that the efficiency and power output are enhanced by quantum discord. This is due to the dependence of the excitation number $\langle n_h^{ss} \rangle$ in Eqs. (18) and (21) on quantum discord $Q(\rho_{12})$. Physically, the quantum discord as a kind of quantum resources contributes to the mean work extracted and thus enhances the performance by increasing power output and efficiency. Further, we note that the oscillations of the curves for the efficiency and power are diminished by increasing quantum discord. The final observation from Fig. 4 is that the quantum entanglement is vanishing at the fixed quantum discord $Q(\rho_{12}) = 0.031$ and thus the engine is fuelled by the reservoirs in separable states. Hence, the presence of quantum discord enhances the performance by increasing efficiency and power and improves the stability by decreasing relative fluctuations of power (see also in the inset of Fig. 5) even when the reservoirs driving quantum heat engines are in the case of separable states where quantum entanglement

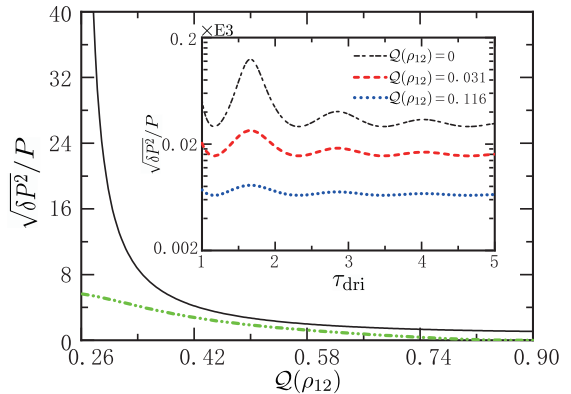


FIG. 5: Coefficient of variation of power (black solid line) as a function of quantum discord for $\tau_{dri} = 0.8$, comparing with its lower bound $\text{csch}[f(\langle\sigma\rangle)]$ (dot-dot-dash line), where $f(x)$ is the inverse function of $x \tanh(x)$ and $x = \langle\sigma\rangle$ denotes the average entropy production in each engine cycle. The parameters are same as Fig. 3. The inset, in which the ordinate axis is logarithmically spaced, shows the coefficient of variation of power as a function of driving time for different values of quantum discord. The other parameters are the same as those in Fig. 4.

is vanishing.

For quantum heat engines where heat and work are stochastic, the fluctuations for the power are required to be considered as they are associated with the machine stability. We consider the coefficient of variation for power, $\sqrt{\delta P^2}/P$, which is equal to the square root of the relative work fluctuations, $\sqrt{\delta w^2}/\langle w \rangle$. This dimensionless coefficient as a function of quantum discord is shown in Fig. 5 with the coefficient as a function of driving time τ_{dri} in the inset. The coefficient of variation for power is monotonically decreased and its oscillation is damped as the quantum discord is increased, thereby showing that the quantum discord can be used to damp the oscillation and the fluctuations of the power output and thereby improves the machine stability.

The total stochastic entropy production σ is distributed according to the probability distribution $p(\sigma)$, with $\sigma(q_h, w) = (\beta_c - \beta_h^{\text{eff}})q_h + \beta_c w$. These distributions for the working system involving time-reversal symmetry satisfy the fluctuation theorems, which can be expressed as $p(\sigma) = p_R(-\sigma)e^\sigma$ [65], with $p_R(-\sigma)$ being the probability distribution of the time-reversed cycle [the clockwise direction in Fig. 2(b)]. These theorems always imply the generalized thermodynamic uncertainty relation for the stochastic work of the form: $\delta w^2/\langle w \rangle^2 \geq \text{csch}^2[f(\langle\sigma\rangle)]$ [53], where $f(x)$ is the inverse function of $x \tanh(x)$. Thus, the coefficient of variation of power should satisfy the relation: $\sqrt{\delta P^2}/P \geq \text{csch}[f(\langle\sigma\rangle)]$, as can be in Fig. 5, where the function $\text{csch}[f(\langle\sigma\rangle)]$ is indicated by the green dot-dot-dash line.

IV. DISCUSSIONS AND CONCLUSIONS

We discuss another model of quantum Otto engine, in which an infinite collection of boson modes and a beam of the correlated pairs of atoms flying sequentially through the cavity act as the hot thermal and cold non-thermal reservoirs, respectively. The inverse temperatures of these two reservoirs are also still denoted by β_h and $\beta_c (> \beta_h)$. In each cycle, the single-mode radiation filed in the optical cavity as the working substance reaches the stationary (thermal) state at the end of the cold (hot) isochoric stroke. In contrast to our previous model where only one atom is weakly coupled to the optical cavity in the hot isochore, in the cold isochoric stroke of the present engine cycle both two atoms pass through the optical cavity. We define $r_1^c = \rho_e^c + \rho_d^c + \rho_{nd}^c$ and $r_2^c = \rho_g^c + \rho_d^c + \rho_{nd}^c$ with $\rho_e^c = \exp(-\beta_c \omega_c) / [2\cosh(\beta_c \omega_c) + 2\cosh(\beta_c \xi)]$, $\rho_g^h = \exp(\beta_c \omega_c) / [2\cosh(\beta_c \omega_c) + 2\cosh(\beta_c \xi)]$, $\rho_d^c = \cosh(\beta_c \xi) / [2\cosh(\beta_c \omega_c) + 2\cosh(\beta_c \xi)]$, and $\rho_{nd}^c = -\sinh(\beta_c \xi) / [2\cosh(\beta_c \omega_c) + 2\cosh(\beta_c \xi)]$. Replacing r_1^h and r_2^h with r_1^c and r_2^c respectively in Eq. (9), the asymptotic stationary solution is $\rho_c^{ss} = (1 - e^{-\beta_c^{\text{eff}} \omega_c}) e^{-\beta_c^{\text{eff}} \omega_c a^\dagger a}$, where β_c^{eff} denotes the effective inverse temperature of the optical cavity. With the detailed balance condition, the ratio of r_1^c / r_2^c becomes $r_1^c / r_2^c = \exp(-\beta_c^{\text{eff}} \omega_c)$, leading to [13]

$$\beta_c^{\text{eff}} = \beta_c - \frac{1}{\omega_c} \ln \frac{1 + e^{\beta_c(\omega_c - \xi)}}{e^{\beta_c \omega_c} + e^{-\beta_c \xi}}, \quad (22)$$

which gives rise to the excitation number $\langle n_c \rangle^{ss} = [\exp(\beta_c^{\text{eff}} \omega_c) - 1]^{-1}$. While keeping in contact with the hot thermal reservoir, the working substance relaxes to the thermal state at the end of the hot isochoric stroke, and its the excitation number is given by $\langle n_h \rangle^{eq} = [\exp(\beta_h \omega_h) - 1]^{-1}$. The key point is that the nonadiabatic factor (17) is only dependent on the system Hamiltonian and driving time. Hence, the work statistics ($\langle w \rangle$ and $\langle \delta w \rangle^2$) and the efficiency (η_{th}) are still given by Eqs. (18), (19) and (21) with replacing $\langle n_h \rangle^{ss}$ and $\langle n_c \rangle^{eq}$ by $\langle n_h \rangle^{eq}$ and $\langle n_c \rangle^{ss}$, respectively. The average work, average heats injection, power output and efficiency (coefficient of performance) are shown in Fig. 6, where we use z^{II} to denote the physical quantity z for the present machine model with the non-thermal cold reservoir. The mode of the thermal machine can be changed if the strength of quantum discord varies; we find that for given control parameters, the quantum-discord-dependent operation mode may be a refrigerator, a heater, or a heat engine, as shown in Fig. 6(a). In addition, it can operate with high efficiency, especially larger than the Carnot efficiency, if quantum discord is large enough, which is consistent with the result in Fig. 3. Figure 6(b) shows that the power and efficiency are improved as quantum discord in the cold isochoric state is increased, which is consistent with Fig. 4. Our additional calculation of the power fluctuations, which is not plotted here, demonstrates that the variance of the power behaves similarly

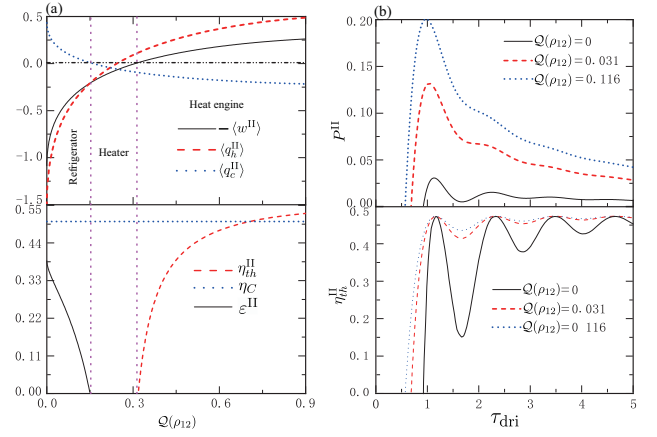


FIG. 6: (a) Work output and heats absorbed by the system (upper panel), and thermodynamic efficiency (lower panel) as a function of quantum discord for $\tau_{\text{dri}} = 0.8$ and $\omega_h = 6$. (b) Output Power (upper panel) and thermodynamics efficiency (lower panel) as a function of driving time for different values of quantum discord at $\omega_h = 3.8$. The other parameters are same as those in Fig. 5.

to corresponding that shown in Fig. 5. We can conclude that the quantum discord (even beyond quantum entanglement) either in the cold or hot heat reservoir is quite beneficial to performance and stability, and even change in the machine mode.

In summary, we have set up a quantum engine working with a single-mode radiation field inside a resonant optical cavity, which is alternatively driven by a thermal reservoir and an out-of-equilibrium reservoir with nonclassical correlations. While the former is composed of boson modes, the latter is realized by sending one of two correlated atoms to weakly interact with the optical cavity. We have investigated the performance parameters characterized by both the power and the thermodynamic efficiency, and machine stability measured by the variation for the power, all of which are dependent on quantum discord associated with nonclassical correlations. We have shown that quantum discord enables the machine as a heat engine to work in the extended regime where the machine without quantum discord may operate as a refrigerator or a heater. Moreover, our quantum Otto engine in the out of equilibrium reservoir with nonclassical correlations enables us to obtain both efficiency and power superior to the counterpart with thermal reservoirs, coinciding with the result obtained from previous models that show superior performance for non-thermal reservoirs, like squeezed ones [20, 21, 64]. Finally, we have demonstrated that the result presented here can be reproduced for another quantum Otto engine model, which is driven by a hot thermal reservoir and a cold non-thermal reservoir by coupling the pair of spin atoms to the optical cavity. Our theoretical results may be useful for using quantum discord as a kind of resources to designing efficient machines in a longer term

respective.

Acknowledgements This work was supported by National Natural Science Foundation (Grant Nos. 11875034, 12175040, and 12161056). J. W. acknowledges financial

support from the Major Program of Jiangxi Provincial Natural Science Foundation. Y.M. acknowledges financial support from the State Key Programs of China under Grant No. 2017YFA0304204.

-
- [1] R. Horodecki, P. Horodecki, M. Horodecki, and K. Horodecki, Quantum entanglement, *Rev. Mod. Phys.* **81**, 865 (2009).
- [2] A. Datta, A. Shaji, and C. M. Caves, Quantum Discord and the Power of One Qubit, *Phys. Rev. Lett.* **100**, 050502 (2008).
- [3] A. Datta and G. Vidal, Role of entanglement and correlations in mixed-state quantum computation, *Phys. Rev. A* **75**, 042310 (2007).
- [4] B. P. Lanyon, M. Barbieri, M. P. Almeida, and A. G. White, Experimental quantum computing without entanglement, *Phys. Rev. Lett.* **101**, 200501 (2008).
- [5] G. M. Andolina, M. Keck, A. Mari, M. Campisi, V. Giovannetti, and M. Polini, Extractable Work, the Role of Correlations, and Asymptotic Freedom in Quantum Batteries, *Phys. Rev. Lett.* **122**, 047702 (2019).
- [6] M. Perarnau-Llobet, K. V. Hovhannisyan, M. Huber, P. Skrzypczyk, N. Brunner, and A. Acín, Extractable Work from Correlations, *Phys. Rev. X* **5**, 041011 (2015).
- [7] A. Sone, Q. Zhuang, C. Li, Y. X. Liu, and P. Cappelaro, Nonclassical correlations for quantum metrology in thermal equilibrium, *Phys. Rev. A* **99**, 052318 (2019).
- [8] C. Wang and Q. H. Chen, Exact dynamics of quantum correlations of two qubits coupled to bosonic baths, *New J. Phys.* **15**, 103020 (2013).
- [9] K. Modi, A. Brodutch, H. Cable, T. Paterek, and V. Vedral, The classical-quantum boundary for correlations: Discord and related measures, *Rev. Mod. Phys.* **84**, 1655 (2012).
- [10] H. Ollivier, and W. H. Zurek, Quantum Discord: A Measure of the Quantumness of Correlations, *Phys. Rev. Lett.* **88**, 017901 (2001).
- [11] M. Ali, A. R. P. Rau, and G. Alber, Quantum discord for two-qubit X states, *Phys. Rev. A* **81**, 042105 (2010).
- [12] L. Henderson and V. Vedral, Classical, quantum and total correlations, *J. Phys. A* **34**, 6899 (2001).
- [13] R. Dillenschneider and E. Lutz, Energetics of quantum correlations, *Europhys. Lett.* **88**, 50003 (2009).
- [14] A. Hewgill, A. Ferraro, and G. De Chiara, Quantum correlations and thermodynamic performances of two-qubit engines with local and common baths, *Phys. Rev. A* **98**, 042102 (2018).
- [15] F. Altintas, Ali Ü. C. Hardal, and Özgür E. M. ustecaplıoğlu, Quantum correlated heat engine with spin squeezing, *Phys. Rev. E* **90**, 032102 (2014).
- [16] G. Alvarado Barrios, F. Albarrán-Arriagada, F. A. Cárdenas-López, G. Romero, and J. C. Retamal, Role of quantum correlations in light-matter quantum heat engines, *Phys. Rev. A* **96**, 052119 (2017).
- [17] X. Wang and J. Wang, The effect of nonequilibrium entropy production on the quantum fisher information and correlations, *Quantum Information Processing* **21**, 1 (2022).
- [18] S. Carnot, *Reflections on the Motive Power of Fire and on Machines Fitted to Develop that Power* (Bachelier, Paris, 1824).
- [19] H. B. Callen, *Thermodynamics and an Introduction to Thermostatistics*, 2nd ed. (Wiley, New York, 1985).
- [20] J. Roßnagel, O. Abah, F. Schmidt-Kaler, K. Singer, and E. Lutz, Nanoscale heat engine beyond the Carnot limit, *Phys. Rev. Lett.* **112**, 030602 (2014).
- [21] J. Klaers, S. Faelt, A. Imamoglu, and E. Togan, Squeezed thermal reservoirs as a resource for a nanomechanical engine beyond the carnot limit, *Phys. Rev. X* **7**, 031044 (2017).
- [22] R. J. de Assis, T. M. de Mendonca, C. J. Villas-Boas, A. M. de Souza, R. S. Sarthour, I. S. Oliveira, and N. G. de Almeida, Efficiency of a Quantum Otto Heat Engine Operating under a Reservoir at Effective Negative Temperatures, *Phys. Rev. Lett.* **122**, 240602 (2019).
- [23] U. Seifert, Stochastic thermodynamics, fluctuation theorems and molecular machines, *Rep. Prog. Phys.* **75**, 126001 (2012).
- [24] K. Sekimoto, *Stochastic Energetics* (Berlin:Springer), 2010.
- [25] J. H. Jiang, B. K. Agarwalla, and D. Segal, Efficiency Statistics and Bounds for Systems with Broken Time Reversal Symmetry, *Phys. Rev. Lett.* **115**, 040601 (2015).
- [26] T. Denzler and E. Lutz, Efficiency fluctuations of a quantum heat engine, *Phys. Rev. Res.* **2**, 032062(R) (2020).
- [27] G. Verley, M. Esposito, T. Willaert, and C. Van den Broeck, The unlikely Carnot efficiency, *Nat. Commun.* **5**, 4721 (2014).
- [28] F. Liu and S. H. Su, Stochastic Floquet quantum heat engines and stochastic efficiencies, *Phys. Rev. E* **101**, 062144 (2020).
- [29] M. N. Ding, Z. C. Tu, and X. J. Xing, Strong coupling thermodynamics and stochastic thermodynamics from the unifying perspective of time-scale separation, *Phys. Rev. Res.* **4**, 013015 (2022).
- [30] V. Holubec, and A. Ryabo, Cycling Tames Power Fluctuations near Optimum Efficiency, *Phys. Rev. Lett.* **121**, 120601 (2018).
- [31] V. Singh and Özgür E. Müstecaplıoğlu, Performance bounds of nonadiabatic quantum harmonic Otto engine and refrigerator under a squeezed thermal reservoir, *Phys. Rev. E* **102**, 062123 (2020).
- [32] J. H. Wang, J. Z. He, and Y. L. Ma, Finite-time performance of a quantum heat engine with a squeezed thermal bath, *Phys. Rev. E* **100**, 052126 (2019).
- [33] Y. N. You and S. W. Li, Entropy dynamics of a dephasing model in a squeezed thermal bath, *Phys. Rev. A* **97**, 012114 (2018).
- [34] G. Manzano, Squeezed thermal reservoir as a generalized equilibrium reservoir, *Phys. Rev. E* **98**, 042123 (2018).
- [35] W. Niedenzu, D. Gelbwaser-Klimovsky, A. G. Kofman, and G. Kurizki, On the operation of machines powered by quantum non-thermal baths, *New. J. Phys.* **18**, 083012 (2016).
- [36] R. J. de Assis, J. S. Sales, J. A. R. da Cunha, and N. G.

- de Almeida, Universal two-level quantum Otto machine under a squeezed reservoir, *Phys. Rev. E* **102**, 052131 (2020).
- [37] G. Manzano, F. Galve, R. Zambrini, and J. M. R. Parrondo, Entropy Production and Thermodynamic Power of the Squeezed Thermal Reservoir, *Phys. Rev. E* **93**, 052120 (2016).
- [38] N. Papadatos, Quantum Stirling heat engine with squeezed thermal reservoir, arXiv:2210.00250v2.
- [39] M. O. Scully, K. R. Chapin, K. E. Dorfman, M. B. Kim, and A. Svidzinsky, Quantum heat engine power can be increased by noise-induced coherence, *Proc. Natl. Acad. Sci. USA* **108**, 15097 (2011).
- [40] H. T. Quan, P. Zhang, and C. P. Sun, Quantum-classical transition of photon-Carnot engine induced by quantum decoherence, *Phys. Rev. E* **73**, 036122 (2006).
- [41] K. Korzekwa, M. Lostaglio, J. Oppenheim, and D. Jennings, The extraction of work from quantum coherence, *New. J. Phys.* **18**, 023045 (2016).
- [42] F. L. S. Rodrigues, G. De Chiara, M. Paternostro, and G. T. Landi, Thermodynamics of Weakly Coherent Collisional Models, *Phys. Rev. Lett.* **123**, 140601 (2019).
- [43] A. Streltsov, G. Adesso, and M. B. Plenio, *Colloquium: Quantum coherence as a resource*, *Rev. Mod. Phys.* **89**, 041003 (2017).
- [44] M. O. Scully, M. S. Zubairy, G. S. Agarwal, and H. Walther, Extracting work from a single heat bath via vanishing quantum coherence, *Science* **299**, 862 (2003).
- [45] T. Guff, S. Daryanoosh, B. Q. Baragiola, and Alexei Gilchrist, Power and efficiency of a thermal engine with a coherent bath, *Phys. Rev. E* **100**, 032129 (2019).
- [46] J. Yi, P. Talkner, and Y. W. Kim, Single-temperature quantum engine without feedback control, *Phys. Rev. E* **96**, 022108 (2017).
- [47] X. Ding, J. Yi, Y. W. Kim, and P. Talkner, Measurement driven single temperature engine, *Phys. Rev. E* **98**, 042122 (2018).
- [48] Z. Y. Lin, S. H. Su, J. Y. Chen, J. C. Chen, and J. F. G. Santos, Suppressing coherence effects in quantum-measurement-based engines, *Phys. Rev. A* **104**, 062210 (2021).
- [49] L. Buffoni, A. Solfanelli, P. Verrucchi, A. Cuccoli, and M. Campisi, Quantum Measurement Cooling, *Phys. Rev. Lett.* **122**, 070603 (2019).
- [50] C. Elouard, D. Herrera-Martí, B. Huard, and A. Auffèves, Extracting Work from Quantum Measurement in Maxwell Demon Engines, *Phys. Rev. Lett.* **118**, 260603 (2017).
- [51] C. Elouard and A. N. Jordan, Efficient quantum measurement engines, *Phys. Rev. Lett.* **120**, 260601 (2018).
- [52] M. N. Bera, A. Riera, M. Lewenstein, and A. Winter, Generalized laws of thermodynamics in the presence of correlations, *Nat. Commun.* **8**, 2180 (2017).
- [53] A. M. Timpanaro, G. Guarnieri, J. Goold, and G. T. Landi, Thermodynamic uncertainty relations from exchange fluctuation theorems, *Phys. Rev. Lett.* **123**, 090604 (2019).
- [54] S.-B. Zheng and G.-C. Guo, Efficient Scheme for Two-Atom Entanglement and Quantum Information Processing in Cavity QED, *Phys. Rev. Lett.* **85**, 2392 (2000).
- [55] S. Hill and W. K. Wootters, Entanglement of a Pair of Quantum Bits, *Phys. Rev. Lett.* **78**, 5022 (1997).
- [56] W. K. Wootters, Entanglement of Formation of an Arbitrary State of Two Qubits, *Phys. Rev. Lett.* **80**, 2245 (1998).
- [57] V. Vedral, Classical Correlations and Entanglement in Quantum Measurements, *Phys. Rev. Lett.* **90**, 050401 (2003).
- [58] S. Luo, Quantum discord for two-qubit systems, *Phys. Rev. A* **77**, 042303 (2008).
- [59] N. Li and S. Luo, Total versus quantum correlations in quantum states, *Phys. Rev. A* **76**, 032327 (2007).
- [60] J. H. Eberly, N. B. Narozhny, J. J. Sanchez-Mondragon, Periodic spontaneous collapse and revival in a simple quantum model, *Phys. Rev. Lett.* **44**, 1323 (1980).
- [61] W. P. Schleich, *Quantum Optics in Phase Space* (Wiley, New York) 2001.
- [62] Z. Y. Fei, J. F. Chen, and Y. H. Ma, Efficiency statistics of a quantum Otto cycle, *Phys. Rev. A* **105**, 022609 (2022).
- [63] T. Denzler and E. Lutz, Efficiency large deviation function of quantum heat engines, *New. J. Phys.* **23**, 075003 (2021).
- [64] Y. Xiao, D. H. Liu, J. Z. He, W. M. Liu, L. L. Yan, and J. H. Wang, Thermodynamics and Fluctuations in Quantum Heat Engines under Reservoir Squeezing, arXiv:2205.13290.
- [65] G. E. Crooks, Nonequilibrium measurements of free energy differences for microscopically reversible Markovian systems, *J. Stat. Phys.* **90**, 1481 (1998).